Stochastic Modeling of Atomizing Spray in a Complex Swirl Injector using Large Eddy Simulation

Sourabh V. Apte
School of Mechanical, Industrial and Manufacturing Engineering, Oregon State University, Corvallis, OR 97331

Krishnan Mahesh
Department of Aerospace Engineering and Mechanics, University of Minnesota, Minneapolis, MN 55455

Michael Gorokhovski
Laboratory of Fluid Mechanics and Acoustics, UMR 5509, CNRS, Ecole Centrale de Lyon, 69131 Ecully Cedex, France

Parviz Moin
Center for Turbulence Research, Stanford University, Stanford, CA 94305

Corresponding Author

Sourabh V. Apte, Oregon State University, 204 Rogers Hall, Corvallis, OR 97331, USA,

email: sva@engr.orst.edu, phone: 541-737-7335, fax: 541-737-2600

Colloquium: SPRAY and DROPLET COMBUSTION

32^{nd} **International Symposium on Combustion**

Word Count (Method M1, manual count)

Abstract: 260 words, Total Main Body Text: 6173 words

Text: 4410 words (346 lines of text), Equations: 228 words (10 equations), Figures and Caption: 950 words (5 figures, Fig. 1 and Fig. 3 are two column figures), References: 542 words (29 references), Acknowledgements: 43 words

Abstract

Large-eddy simulation of an atomizing spray issuing from a gas-turbine injector is performed. The filtered Navier-Stokes equations with dynamic subgrid scale model are solved on unstructured grids to compute the swirling turbulent flow through complex passages of the injector. The collocated grid, incompressible flow algorithm on arbitrary shaped unstructured grids developed by Mahesh *et al.* (J. Comp. Phy., 2004, **197**, 215–240) is used in the present work. A Lagrangian point-particle formulation with a stochastic model for droplet breakup is used for the liquid phase. Following Kolmogorov's concept of viewing solid particle-breakup as a discrete random process, the droplet breakup is considered in the framework of uncorrelated breakup events, independent of the initial droplet size. The size and number density of the newly produced droplets is governed by the Fokker-Planck equation for the evolution of the *pdf* of droplet radii. The parameters of the model are obtained dynamically by relating them to the local Weber number and resolved scale turbulence properties. A hybrid particle-parcel is used to represent the large number of spray droplets. The predictive capability of the LES together with Lagrangian droplet dynamics models to capture the droplet dispersion characteristics, size distributions, and the spray evolution is examined in detail by comparing it with the spray patternation study for the gas-turbine injector. The present approach is computationally efficient and captures the global features of the fragmentary process of liquid atomization in complex configurations.

Key words: Sprays, LES, complex geometries, droplet breakup, stochastic models

1 Introduction

Liquid spray atomization plays a crucial role in analyzing the combustion dynamics in many propulsion related applications. This has led researchers to focus on modeling of droplet formation in numerical investigations of chemically reacting flows with sprays. In the traditional approach for spray computation, the Eulerian equations for gaseous phase are solved along with a Lagrangian model for dropet transport with two-way coupling of mass, momentum, and energy exchange between the two phases [1]. The standard approach is to first perform spray patternation studies for the injector used in combustion chambers and measure the size distributions at various cross-sections from the injector. These distributions are then used as an *input* to a numerical simulation which then computes the secondary atomization of the injected droplets. The secondary atomization is typically modeled by standard deterministic breakup models based on Taylor Analogy Breakup (TAB) [2], or wave [3] models. However, this requires performance of experimental tests for any new injector design which can be very costly.

Development of numerical approaches for direct simulations of the primary atomization of a liquid jet or sheet is necessary. However, such approaches also require significant computational effort. Such numerical schemes capture the complex interactions and instabilities near the gas-liquid interface, formation of ligaments and their disintegration into droplets. Considerable advances have been made in this area [4–6]. The predictive capability of such schemes may be strongly influenced by the grid resolutions used and capabilities for realistic injector geometries are still under development.

Majority of spray systems in propulsion applications involve complex geometries and highly unsteady, turbulent flows near the injector. The numerical models for spray calculations should be able to accurately represent droplet deformation, breakup, collision/coalescence, and dispersion

due to turbulence. Simulations involving comprehensive modeling of these phenomena are rare. Engineering prediction of such flows relies predominantly on the Reynolds-averaged Navier-Stokes equations (RANS) [7,8]. However, the large-eddy simulation (LES) technique has been convincingly shown to be superior to RANS in accurately predicting turbulent mixing in simple [9], and realistic [10–12] combustor geometries. It was shown that LES captures the gas-phase flow physics accurately in swirling, separated flows commonly observed in propulsion systems. Recently, Apte *et al.* [13] have shown good predictive capability of LES in swirling, particle-laden coaxial combustors. The particle-dispersion characteristics were well captured by the Eulerian-Lagrangian formulation.

In the present work, LES together with a stochastic subgrid model for droplet atomization is used for simulation of spray evolution in a real gas-turbine injector geometry. Modeling of the complexities of the atomization process is based on a stochastic approach. Here, the details of the ligament formation, liquid sheet/jet breakup in the near injector region are not computed in detail, but their global features are modeled in a statistical sense. Following Kolmogorov's concept of viewing solid particle-breakup as a discrete random process [14], atomization of liquid drops at high relative liquid-to-gas velocity is considered in the framework of uncorrelated breakup events, independent of the initial droplet size. Gorokhovski and Saveliev [15] reformulated Kolmogorov's discrete model of breakup in the form of a differential Fokker-Planck equation for the *pdf* of droplet radii. The probability to break each parent drop into a certain number of parts is assummed independent of the parent-drop size. Using central limit theorem, it was pointed out that such a general assumption leads to a log-normal distribution of particle size in the long-time limit. This approach was further extended in the context of large-eddy simulations of the gas-phase by Apte *et al.* [16] and validated for spray evolution in simplified Diesel engine configuration.

In this work, the stochastic breakup model is applied to simulate a spray evolution from a realistic

pressure-swirl injector to evaluate the predictive capability of the model together with the LES framework. As the first step, cold flow simulation with stochastic model for secondary atomization is performed. This study thus isolates the problem of liquid atomization in pressure-swirl injectors typically used in gas-turbine engines and serves as a systematic validation study for multiphysics, reacting flow simulations in realistic combustors [12].

In subsequent sections, the mathematical formulations for the large-eddy simulation of the gaseous-phase and subgrid modeling of the liquid phase are summarized. Next, the stochastic model for liquid drop atomization is discussed together with a hybrid particle-parcel algorithm, based on the original parcels approach proposed by O'Rourke and Bracco [17], for spray simulations. The numerical approach is then applied to compute unsteady, swirling flows in a complex injector geometry and the results are compared with available experimental data on spray patternation studies.

2 Mathematical Formulation

The governing equations used for the gaseous and droplet phases are described briefly. The droplets are treated as point-sources and influence the gas-phase only through momentum-exchange terms [13].

2.1 Gas-Phase Equations

The three-dimensional, incompressible, filtered Navier-Stokes equations are solved on unstructured grids with arbitrary elements. These equations are written as

$$\frac{\partial \overline{u_i}}{\partial t} + \frac{\partial \overline{u}_i \overline{u}_j}{\partial x_j} = -\frac{\partial \phi}{\partial x_i} + \frac{1}{Re_{ref}} \frac{\partial^2 \overline{u}_i}{\partial x_j x_j} - \frac{\partial q_{ij}}{\partial x_j} + \overline{\dot{S}_i} \tag{1}$$

where q_{ij} denotes the anisotropic part of the subgrid-scale stress tensor, $\overline{u_i u_j} - \overline{u}_i \overline{u}_j$, and the overbar indicates filtered variables. The dynamic Smagorinsky model is used for q_{ij} [18]. Equation (1) is non-dimensionalized by the reference length, velocity, and density scales, L_{ref}, U_{ref}, ρ_{ref}, respectively. The reference Reynolds number is defined as $Re_{ref} = \rho_{ref} L_{ref} U_{ref} / \mu_{ref}$. The source-term $\overline{\dot{S}_i}$ in the momentum-equations represent the 'two-way' coupling between the gas and particle-phases and is given by

$$\overline{\dot{S}_i} = -\sum_k \mathcal{G}_\sigma(\mathbf{x}, \mathbf{x}_p) \frac{\rho_p^k}{\rho_{ref}} V_p^k \frac{du_{pi}^k}{dt} \tag{2}$$

where the subscript p stands for the droplet phase. The $\sum_k$ is over all droplets in a computational control volume. The function $\mathcal{G}_\sigma$ is a conservative interpolation operator with the constraint $\int_{\mathrm{V_{cv}}} \mathcal{G}_\sigma(\mathbf{x}, \mathbf{x}_p) dV = 1$ [13], where $\mathrm{V_{cv}}$ is the volume of the grid cell and $V_p{}^k$ is the volume of the k^{th} droplet.

2.2 Liquid-Phase Equations

Droplet dynamics are simulated using a Lagrangian point-particle model. It is assumed that (1) the density of the droplets is much greater than that of the carrier fluid, (2) the droplets are dispersed, (3) the droplets are much smaller than the LES filter width, (4) droplet deformation effects are small, and (5) motion due to shear is negligible. Under these assumptions, the Lagrangian equations governing the droplet motions become [19]

$$\frac{d\mathbf{x}_p}{dt} = \mathbf{u}_p; \quad \frac{d\mathbf{u}_p}{dt} = \frac{1}{\tau_p} (\mathbf{u}_{g,p} - \mathbf{u}_p) + \left(1 - \frac{\rho_g}{\rho_p}\right) \mathbf{g} \tag{3}$$

where $\mathbf{x}_p$ is the position of the droplet centroid, $\mathbf{u}_p$ denotes the droplet velocity, $\mathbf{u}_{g,p}$ the gas-phase velocities interpolated to the droplet location, ρ_p and ρ_g are the droplet and gas-phase densities,

and $\mathbf{g}$ is the gravitational acceleration. The droplet relaxation time scale (τ_p) is given as [19]

$$\tau_p = \frac{\rho_p d_p^2}{18\mu_g} \frac{1}{1 + aRe_p^b}, \tag{4}$$

where d_p is the diameter and $Re_p = \rho_g d_p |\mathbf{u}_{g,p} - \mathbf{u}_p|/\mu_g$ is the droplet Reynolds number. The above correlation is valid for $Re_p \leq 800$. The constants $a = 0.15, b = 0.687$ yield the drag within 5% from the standard drag curve.

Note that some of the above assumptions for the point-particle approach are not valid very close to the injector. The droplets may undergo deformation [20], collision, and coalescence. However, as a first step these effects are not considered and further investigations are needed to evaluate their influence.

2.3 Stochastic Modeling of Droplet Breakup

As the physics of primary and secondary atomization are not well understood even in simple and canonical flow configurations, a heuristic approach based on stochastic modeling is followed in order to reduce the number of tuning parameters in an atomization model. A stochastic breakup model capable of generating a broad range of droplet sizes at high Weber numbers has been developed [6,15,16]. In this model, the characteristic radius of droplets is assumed to be a time-dependent stochastic variable with a given initial size-distribution. For very large Weber numbers, there is experimental evidence indicating the fractal nature of atomization process [21,22] wherein large droplets can directly disintegrate into tiny droplets. The stochastic nature of this process is modeled by the present approach. The breakup of parent drops into secondary droplets is viewed as the temporal and spatial evolution of this distribution function around the parent-droplet size

according to the Fokker-Planck (FP) differential equation

$$\frac{\partial T(x,t)}{\partial t} + \nu(\xi)\frac{\partial T(x,t)}{\partial x} = \frac{1}{2}\nu(\xi^2)\frac{\partial^2 T(x,t)}{\partial x^2}, \tag{5}$$

where the breakup frequency (ν) and time (t) are introduced. The moments $\langle\xi\rangle = \int_{-\infty}^{0}\xi S(\xi)d\xi$ and $\langle\xi^2\rangle = \int_{-\infty}^{0}\xi^2 S(\xi)d\xi$ are the two parameters of the model that need closure. Here, $T(x,t)$ is the distribution function for $x = \ln(r)$, and r is the droplet radius. Breakup occurs when $t > t_{bu} = 1/\nu$ and $r > r_{cr}$, the critical radius of the droplet. Following the arguments of scale similarity analogous to the turbulence cascade behavior at large Reynolds numbers, Gorokhovski and Saviliev [15] looked at the long-time behavior of the droplet breakup. They showed that the initial delta-function for the logarithm of radius of the j^{th} primary droplet evolves into a steady state distribution that is a solution to the Fokker Planck equation [15,16]

$$T_j(x,t+1) = \frac{1}{2}\left[1 + \mathrm{erf}\left(\frac{x - x_j - \langle\xi\rangle}{\sqrt{2\langle\xi^2\rangle}}\right)\right]. \tag{6}$$

This long time behavior of the distribution is characterized by the dominant mechanism of breakup. Improvements to the model, wherein presence of a liquid core near the injector is taken into account [23], have been proposed, however, in the present work an initial dirac-delta function is assumed at the injector surface.

The value of the breakup frequency and the critical radius of breakup are obtained by the balance between the aerodynamic and surface tension forces. The critical (or maximum stable) radius for breakup is then given as $r_{cr} = We_{cr}\sigma/(\rho_g u_{r,j}^2)$ where $|u_{r,j}|$ is the relative velocity between the gas and droplet, σ the surface tension coefficient, We_{cr} the critical Weber number, which is assumed to be on the order of six over a wide range of Ohnesorge numbers. For highly turbulent flows, however, the instantaneous value of Kolmogorov scale (η) is often less than the droplet size and the entire spectrum of turbulent kinetic energy can contribute to the stretching and disintegration

of the droplet. In this case, the critical radius should be obtained as a balance between the capillary forces and turbulent kinetic energy supplied to the liquid droplet. Accordingly, the relative droplet-to-gas velocity is estimated from the mean viscous dissipation and Stokes time scale (τ_{st}) as $|u_{r,j}^2| \approx \epsilon\tau_{st}$ [24]. Using this relative velocity, the critical radius of breakup becomes

$$r_{cr} = \left(\frac{9}{2}\frac{We_{cr}\sigma\nu_{lam}}{\epsilon\rho_\ell}\right)^{1/3}, \tag{7}$$

where ν_{lam} is the kinematic viscosity, ρ_ℓ is the liquid density, and ϵ is the viscous dissipation rate. In the present LES study, the viscous dissipation can be obtained dynamically form the resolved scale energy flux. The breakup frequency is obtained following the analogy with expressions used for aerodynamic breakup and utilizing the relative velocity ($|u_{r,j}|$) from above

$$t_{bu} = B\sqrt{\frac{\rho_l}{\rho_g}}\frac{r_j}{|u_{r,j}|}, \tag{8}$$

where r_j is the radius of parent drop and $B = \sqrt{1/3}$ [2,25].

If the breakup criterion ($t > t_{bu}$ and $r > r_{cr}$) for a parent droplet is satisfied, secondary droplets are sampled from the analytical solution (Eq. 6) corresponding to the breakup time-scale. The parameters encountered in the FP equation ($\langle\xi\rangle$ and $\langle\xi^2\rangle$) are computed by relating them to the local Weber number for the parent drop, thereby accounting for the capillary forces and turbulent properties. Apte *et al.* [16] assumed that in the intermediate range of scales between the parent drop element (large Weber number) and the maximum stable droplet (critical Weber number) there exists no preferred length scale, following the fractal nature of atomizing spray [22]. This closely resembles the inertial range of the energy cascade process in homogeneous turbulence at high Reynolds numbers. Analogously, assuming $u_{r,j}^3/r_j = u_{r,cr}^3/r_{cr}$, one obtains

$$\frac{r_{cr}}{r_j} = \left(\frac{We_{cr}}{We_j}\right)^{3/5} \Longrightarrow \langle \ln\alpha\rangle \equiv \langle\xi\rangle = K\ln\left(\frac{We_{cr}}{We_j}\right), \tag{9}$$

where $u_{r,cr}$ is the relative velocity at which disruptive forces are balanced by capillary forces (similar to turbulent velocity scale of the smallest eddies) and the constant K is of order unity (~ 0.6). This gives expression for one of the parameters $\langle\xi\rangle$.

Furthermore, from the Einstein's theory of Brownian motion, the diffusion coefficient in the Fokker-Planck equation is known to be the energy of Brownian particles multiplied by their mobility. The drift velocity is presented in the form of drag force times the mobility. The ratio of diffusion to drift velocity is given by the ratio of energy to drag force. In the breakup process, the energy in Einstein's theory is associated with the disruptive energy while the force is associated with the capillary force on the droplet. Normalized by the length scale of the parent drop, this ratio is characterized by the Weber number. Considering the Fokker Planck equation (Eq. 5), the diffusion to drift velocity ratio is scaled by $-\langle\xi^2\rangle/\langle\xi\rangle$. Then it is assumed that

$$-\frac{\langle\xi\rangle}{\langle\xi^2\rangle} \equiv -\frac{\langle \ln\alpha\rangle}{\left\langle \ln^2\alpha\right\rangle} = We_j^{-1}. \tag{10}$$

This relationship gives the maximum dispersion of newly produced droplet sizes. Thus, both the parameters in the Fokker Planck equation are obtained dynamically by computing the local value of We_j, and knowing We_{cr}.

Once new droplets are created, the product droplet velocity is computed by adding a factor $\mathbf{w}_{bu}$ to the primary drop velocity. This additional velocity is randomly distributed in a plane normal to the relative velocity vector between the gas-phase and parent drop, and the magnitude is determined by the radius of the parent drop and the breakup frequency, $|\mathbf{w}_{bu}| = r\nu$. This modification of newly formed droplets follows the physical picture of parent droplets being torn apart by aerodynamic forces giving momentum to the newly formed droplets in the direction normal to the relative velocity between the gas-phase and parent drops [2].

As new droplets are formed, parent droplets are destroyed and Lagrangian tracking in the physical space is continued till further breakup events. In the present work, the liquid spray is injected at atmospheric pressure and temperatures. The rates of evaporation are very small and droplet evaporation is neglected.

2.4 Subgrid Scale Modeling

In LES of droplet-laden flows, the droplets are presumed to be *subgrid*, and the droplet-size is smaller than the filter-width used. The gas-phase velocity field required in Eq. (3) is the total (unfiltered) velocity, however, only the filtered velocity field is computed in Eqs. (1). The direct effect of unresolved velocity fluctuations on droplet trajectories depends on the droplet relaxation time-scale, and the subgrid kinetic energy. Considerable progress has been made in reconstructing the unfiltered velocity field by modeling the subgrid scale effects on droplet dispersion. Bellan [26] provides a good review on this topic in the context of spray modeling. Majority of the works related to subgrid scale effects on droplet motion have been performed for dilute loadings, wherein the droplets are either assumed smaller than the LES filter size or the Kolmogorov length scale. For dense spray systems, droplet dispersion and droplet interactions with subgrid scale turbulence are not well understood. In addition, In realistic configurations the droplet sizes very close to the injector can be on the order of the grid size used for LES computations.

Recently, Pozorski and Apte [27] performed a systematic study of the direct effect of subgrid scale velocity on particle motion for forced isotropic turbulence. It was shown that, in poorly resolved regions, where the subgrid kinetic energy is more than 30%, the effect on droplet motion is more pronounced. A stochastic model reconstructing the subgrid-scale velocity in a statistical sense was developed [27]. However, in well resolved regions, where the amount of energy in the subgrid scales

is small, this direct effect was not strong. In the present work, the direct effect of subgrid scale velocity on the droplet motion is neglected. However, note that the droplets *do feel* the subgrid scales through the subgrid model that affects the resolved velocity field. For well-resolved LES of swirling, separated flows with the subgrid scale energy content much smaller than the resolved scales, the direct effect was shown to be small [13].

3 Numerical Method

The computational approach is based on a co-located, finite-volume, energy-conserving numerical scheme on unstructured grids [10] and solves the incompressible Navier-Stokes equations. The velocity and pressure are stored at the centroids of the control volumes. The cell-centered velocities are advanced in a predictor step such that the kinetic energy is conserved. The predicted velocities are interpolated to the faces and then projected. Projection yields the pressure potential at the cell-centers, and its gradient is used to correct the cell and face-normal velocities. A novel discretization scheme for the pressure gradient was developed by Mahesh *et al.* [10] to provide robustness *without numerical dissipation* on grids with rapidly varying elements. This algorithm was found to be imperative to perform LES at high Reynolds numbers in realistic combustor geometries and is essential for the present configuration. This formulation has been shown to provide very good results for both simple and complex geometries [10–12].

In addition, for two-phase flows the particle centroids are tracked using the Lagrangian framework. The particle equations are integrated using third-order Runge-Kutta schemes. Owing to the disparities in the flowfield time-scale and the droplet relaxation time (τ_p) sub-cycling of the droplet equations may become necessary. After obtaining the new droplet positions, the droplets are relocated, droplets that cross interprocessor boundaries are duly transferred, boundary conditions on

droplets crossing boundaries are applied, source terms in the gas-phase equation are computed, and the computation is further advanced. Solving these Lagrangian equations thus requires addressing the following key issues: (i) efficient search for locations of droplets on an unstructured grid, (ii) interpolation of gas-phase properties to the dropletlocation for arbitrarily shaped control volumes, (iii) inter-processor droplet transfer. An efficient Lagrangian framework was developed which allows tracking millions of droplet trajectories on unstructured grids [13,16].

Hybrid Droplet-Parcel Algorithm for Spray Computations: Performing spray breakup computations using Lagrangian tracking of each individual droplet gives rise to a large number of droplets ($\approx$ 20-50 million) in localized regions very close to the injector. Simulating all droplet trajectories gives severe load-imbalance due to presence of droplets on only a few processors. On the other hand, correct representation of the fuel vapor distribution obtained from droplet evaporation is necessary to capture the dynamics of spray flames. In their pioneering work, O'Rourke and Bracco [17] used a 'discrete-parcel model' to represent the spray drops. A parcel or computational particle represents a group of droplets, N_{par}, with similar characteristics (diameter, velocity, temperature). Typically, the number of computational parcels tracked influences the spray statistics predicted by a simulation.

The original work of O'Rourke and co-workers [2,17] inject parcels from the injector, resulting in much fewer number of tracked computational particles. In this work, the parcels model is further extended to a hybrid particle-parcel scheme [16]. The basic idea behind the hybrid-approach is as follows. At every time step, droplets of the size of the spray nozzle are injected based on the fuel mass flow rate. New droplets added to the computational domain are pure drops ($N_{par} = 1$). These drops are tracked by Lagrangian particle tracking and undergo breakup according to the stochastic model creating new droplets of smaller size. As the local droplet number density exceeds a prescribed threshold, all droplets in that control volume are collected and grouped into bins

corresponding to their size. The droplets in bins are then used to form a parcel by conserving mass. Other properties of the parcel are obtained by mass-weighted averaging from individual droplets in the bin. The number of parcels created would depend on the number of bins and the threshold value used to sample them. A parcel thus created then undergoes breakup according to the above stochastic sub-grid model, however, does not create new parcels. On the other hand, N_{par} is increased and the diameter is decreased by mass-conservation.

This strategy effectively reduces the total number of computational particles in the domain. Regions of low number densities are captured by individual droplet trajectories, giving a more accurate spray representation.

4 Computational Details

Figure 1 shows a schematic of the computational domain used for the spray patternation study of a realistic Pratt and Whitney injector. The experimental data set [28,29] was obtained by mounting the actual injector in a cylindrical plenum through which gas with prescribed mass-flow rate was injected. Figure (1b) shows a cut through the symmetry plane ($Z/L_{ref} = 0$) of the computational domain along with the mesh and boundary conditions used. For this case, 3.2M grid points are used with high resolution near the injector. The grid elements are a combination of tetrahedra, prisms, wedges, and hexahedra to represent complex geometric passages inside the injector. Grid refinement study for LES of single phase flow has been performed for different cases in complex configurations [10,11]. The grid resolution for the present case was decided based on these validation studies.

Air from the inlet plenum goes through the central core, guide, and outer swirlers to create highly unsteady multiple swirling jets. The domain decomposition is based on the optimal performance

of the Eulerian gas-phase solver on 96 processors. Brankovic *et al.* [28] provide details of the experimental measurement techniques and inflow conditions for a lower pressure drop across the fuel nozzle. The inflow conditions in the present study are appropriately scaled to a higher pressure drop providing the air mass flow rate of 0.02687 kg/s. The flow Reynolds number based on the inlet conditions is $14,960$. A uniform mean inflow velocity was specified at the inlet without any turbulent fluctuations. In the present case, the downstream cylindrical plenum is open to atmosphere. The air jet coming out of the nozzle thus entrains air from the surrounding. Entrained flow along the surface of the downstream plenum was modeled as a radially inward velocity along the entire plenum surface. The experimental data profiles at different cross-sections were integrated at each station to obtain the total flow rate at those locations. Knowing the net inflow rate, the entrained mass at each of the entrainment boundaries was estimated and assigned to the calculation. This modeling approach for entrained flow is subject to experimental verification, however, was shown to have little impact on the predicted flowfield [28]. No-slip conditions are specified on the wall. Convective boundary conditions are applied at the exit section by conserving the global mass flow rate through the computational domain. and experimentally measured radial entrainment rate is applied on the cylindrical surface of the computational domain downstream of the injector.

Liquid fuel is injected through the filmer surface which forms an annular ring near the outer swirler. In the symmetry plane this is indicated by two points on the edge of the annular ring. The ratio of the liquid to air mass flow rates at the inlet is fixed at 0.648. The liquid film at the filmer surface is approximated by injecting uniform size large drops of the size of the annular ring thickness. These drops are convected downstream by the swirling air and undergo breakup according to the stochastic model. The velocity of each droplet is specified based on the velocity of the liquid film. A large number of droplets are created in the vicinity of the injector due to breakup. The location of droplet injection around the annular ring is chosen using uniform random

distribution. This discrete representation of the film near the injector surface may not represent the physics of ligament formation and film breakup. However, the statistical nature of droplet formation further away from the injector is of interest in the present study and is well captured by the stochastic model together with LES of the air flow.

With the hybrid approach, the total number of computational particles tracked at stationary state is around 3.5M and includes around $150,000$ parcels. Together these represent aproximately 13M droplets. The computations were performed on the IBM cluster at the San Diego Supercomputing center.

5 Results and Discussion

Figures 2a,b show the instantaneous snapshots of the axial velocity contours in the $Z/L_{ref} = 0$ symmetry plane and in cross-section $X/L_{ref} = 1.1$. Figures 2c,d show the corresponding snapshots for spray droplets (white dots). The swirling air jet from the core swirler enters the dump region and forms a recirculation zone. Jets from guide and outer swirlers interact with the core flow. The swirling air jets entering the sudden expansion region create radially spreading conical jets with a large recirculation region just downstream of the injector. A complex vortex break down phenomenon is observed and its accurate prediction is necessary to correctly represent the injector flow. The swirl strength decays further away from the injector due to viscous dissipation. The scatter plot of the spray droplets show dense spray regimes close to the injector which become dilute further away. The parent droplets are injected at the edge of the annular ring. These droplets are carried by the swirling flow and form a conical spray. The concentration of the spray droplets is high on the edge of the recirculation region. The strong relative motion between the large inertial droplets near the injector and the fluid flow leads to breakup and generation of smaller droplets.

The droplets spread radially outward and swirl around the injector axis as they move downstream.

Figures 3a,b compare the LES predictions to the available experimental data of radial variations of mean axial and swirl velocity at different axial locations. The numerical results are azimuthally averaged. The predictions from our simulation are in close agreement with the experimental data [29]. The size and evolution of the recirculation region is well captured as indicated by the axial velocity predictions. The swirl strength decays downstream of the injector. Small disagreement at $X/L_{ref} = 2.1$ is partly related to the coarse grid resolution used away from the injector. It should be noted that the amount of swirl generator by the injectors determines the size of the recirculation zone. Good agreement of the axial and swirl velocities indicate that LES with dynamic sgs model can capture the vortex break-down phenomenon accurately in complex geometries. Also shown are the corresponding predictions using the standard $k - \epsilon$ model on the present grid. The unsteady RANS solutions are in agreement with the LES and experimental data very close to the injector, however, degrade rapidly further away, showing limitations of the turbulence model. RANS predictions of the flow through the same injector at different conditions [28] show similar trends. Improved predictions using advanced RANS models can be obtained, however, the superiority of LES is clearly demonstrated. Any artificial dissipation or inaccurate numerics gives faster decay of the swirl velocities and incorrect size of the recirculation region, further emphasizing the importance of *non-dissipative* numerical schemes for LES.

Figures 4a,b compare the radial variation of liquid mass-flowrates using LES and the stochastic model to the experimental data at two different cross-sections. The flow rates are presented as the ratio of the effective to the integrated flow rate. The effective flow rate is defined as the flow rate the patternator would record if the fuel flux was uniform at the local value. This normalization inherently carries the ratio of the total cross-sectional area to the area of the local patternator holes. The LES results are generally in good agreement with the experiments. Average droplet

sizes at two axial location from the injector wall have been measured using the Malvern line of sight technique [29]. The Sauter mean diameters averaged over the cross-section at these two axial locations are predicted within 5% of the experimental values.

Figures 5a,b compare the mass-based size-distribution function compared with the experimental data at two different cross-sections from the injector. It is observed that the predicted distribution functions agree with experimental observations for large-size droplets. However, the simulations predict larger mass of small size droplets compared with the experimental data. This is attributed to the lack of collision/coalescence models in the present simulation. Also, small size droplets can easily evaporate even at low temperatures and the present simulations do not consider this effect. In addition, the initial droplet size at the injector nozzle is assumed to be a constant, whereas it may vary depending on the local conditions governing primary atomization. Models taking into account the presence of a liquid core near the injector can be incorporated to better capture the recirculation regions. A dirac-delta function was used to inject large drops from the injector surface and a better representation of these initial conditions can improve the predictions [23]. Further improvements to the model can also be obtained by modeling the primary breakup regime very close to the injector. An investigation with inclusion of collision models as well as using a size distribution at the inlet should be performed in order to investigate uncertainties in model predictions. However, the overall predictions of the LES methodology together with a simple stochastic breakup model of liquid atomization are in good agreement with experiments. The dispersion of droplets in an unsteady turbulent flow is well represented when the flowfield is computed using LES.

6 Summary and Conclusions

A large-eddy simulation of an atomizing spray issuing from a gas-turbine injector is performed corresponding to the spray patternation study of an injector used in a Pratt and Whitney combustor. The filtered Navier-Stokes equations with dynamic subgrid scale models are solved on unstructured grids to compute the swirling turbulent flow through complex passages of the injector. A Lagrangian point-particle formulation with stochastic models for droplet breakup is used for the liquid phase. The atomization process is viewed as a discrete random process with uncorrelated breakup events, independent of the initial droplet size. The size and number density of the newly produced droplets is governed by the Fokker-Planck equation for the evolution of the *pdf* of droplet radii. The parameters of the model are obtained dynamically by relating them to the local Weber number and resolved scale turbulence properties. It is assumed that for large Weber numbers there exists no preferred length scale in the intermediate range of scales between the parent drop element and the maximum stable droplet, following the fractal nature of atomizing spray [21,22]. A hybrid particle-parcel approach is used to represent the large number of spray droplets. The swirling, separated regions of the flow in this complex configuration are well predicted by the LES. The droplet mass fluxes and size distributions predicted are within the experimental uncertainties further away from the injector. The present approach, however, overpredicts the number density of small size droplets which can be attributed to the lack of coalescence modeling. In addition, the primary breakup regime very close to the injector was not simulated. Models taking into account the presence of a liquid core near the injector [23] can be incorporated to better capture the recirculation regions. However, with present stochastic approach the droplet dispersion characteristics are well captured. The global features of the fragmentary process of liquid atomization resulting in a conical spray are well represented by the present LES in realistic injector geometry. This stochastic modeling approach has been used to perform full scale simulations of turbulent spray

combustion in a real Pratt and Whitney combustion chamber [12]

Acknowledgments

Support for this work was provided by the United States Department of Energy under the Advanced Scientific Computing (ASC) program. The computer resources at San Diego Supercomputing Center are greatly appreciated. We are indebted to Dr. Gianluca Iaccarino and the combustor group at Pratt and Whitney.

References

[1] Dukowicz, J.K., *J. Comp. Phy.*, 35:229 (1980).

[2] O'Rourke P.J., and Amsden, A.A., *SAE Technical Paper*, 87-2089 (1987).

[3] Reitz, R.D., *Atom. Spray Tech.*, 3: 307, (1987).

[4] Tanguy, S., and Berlemont, A. *Int. J. Mult. Flow*, 31:1015–1035 (2005).

[5] Menard, T., Tanguy, S., and Berlemont, A. *Int. J. Mult. Flow*, 33: 510–524 (2007).

[6] Gorokhovski, M., and Herrmann, M., *Ann. Rev. Fl. Mech.* 40:343–366 (2008).

[7] Ruger, M., Hohmann, S., Sommerfeld, M., and Kohnen, G., *Atom. Sprays*, 10:47–81 (2000).

[8] Schmidt, D.P., Chiappetta, L.M., Goldin, G.M., Madabhushi, R.K., *Atom. Sprays*, 13:373–394 (2003).

[9] Pierce, C. and Moin, P., *The progress variable approach for large eddy simulation of turbulent combustion*, TF-Report 80, Stanford University, Stanford, California (2001).

[10] Mahesh, K., Constantinescu, G., and Moin, P., *J. Comp. Phy.*, 197, 215–240 (2004).

[11] Mahesh, K., Constantinescu, G. Apte, S.V., Iaccarino, G., Ham, F., and Moin, P., *ASME J. App. Mech.*, 7:374–381 (2006).

[12] Moin, P., and Apte, S.V. *AIAA J.* 44, 698–710 (2006).

[13] Apte, S. V., Mahesh, K., Moin, P., and Oefelein, J.C., *Int. J. Mult. Flow* 29:1311–1331 (2003a).

[14] Kolmogorov A.N., *Dokl. Akad. Nauk. SSSR*, XXXI, 2: 99–101 (1941).

[15] Gorokhovski, M., Saveliev, V., *Phys. Fluids* 15:184–92 (2005).

[16] Apte, S. V., Gorokhovski, M., and Moin, P., *Int. J. Mult. Flow* 29:1503–1522 (2003b).

[17] O'Rourke, P. and Bracco, F., *Proceedings of the Institution of Mechanical Engineers*, 9:101–106 (1980).

[18] Germano, M., Piomelli, U., Moin, P., and Cabot, W.H., *Phys. Fluids* A 3(7) (1991).

[19] Crowe, C., Sommerfeld, M., and Tsuji, Y. *Multiphase flows with droplets, and particles*, CRC Press (1998).

[20] Apte, S. V., Helenbrook, B., and Moin, P., *Large-eddy simulation of swirling particle-laden flows in a coaxial-jet combustor*. Proceedings of the 16^{th} Conference of Liquid Atomization and Spray Systems, (2003).

[21] Shavit U, and Chigier N. *J. Atom. Sprays* 5:525–43, 1995.

[22] Zhou, W. X. and Yu, Z. H., *Phys. Rev. E.*, 63: 016302, 2000.

[23] Gorokhovski M, Jouanguy J, and Chtab A., *Simulation of air-blast atomization: 'floating guard' statistic particle method for conditioning of LES computation; stochastic models of break-up and coalescence.* Proc. Int. Conf. Liq. Atom. Spray Syst., 10th (ICLASS-2006), 2006.

[24] Kuznezov V.R., and Sabel'nikov V.A., *Turbulence and Combustion*, Hemisphere Publishing Corporation, New York (1990).

[25] Faeth, G.M., Hsiang, L.P., and Wu P.K., *Int. J. Mult. Flow*, 21: 99–127 (1995).

[26] Bellan, J., *Perspectives on large eddy simulations for sprays: issues and solutions* Proc. Int. Conf. Liq. Atom. Spray Syst., 8th (ICLASS-2000), 2000.

[27] Pozorski, J., and Apte, S.V., *Int. J. Mult. Flow*, accepted, pending revisions.

[28] Brankovic, A., McKinney, R., Ouyang, H., Porter, L., Kennedy, J., Madabhushi, R., and Colket, M., *Comparison of measurements and predictions of Flow in a gas turbine engine fuel nozzle*, AIAA-2000-0331, 2000.

[29] McKinney, R., Madabhushi, R.K., and Syed, S., *private communication* (2002).

List of Figures

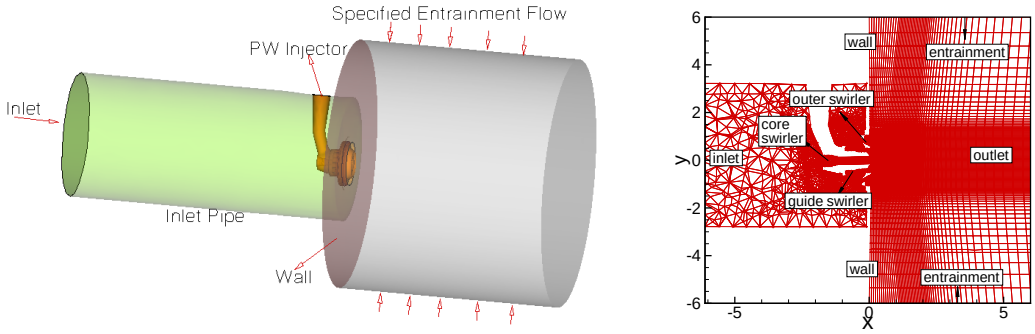

Fig. 1. The computational domain: (a) schematic of entire region, (b) unstructured grid near the injector in the symmetry plane.

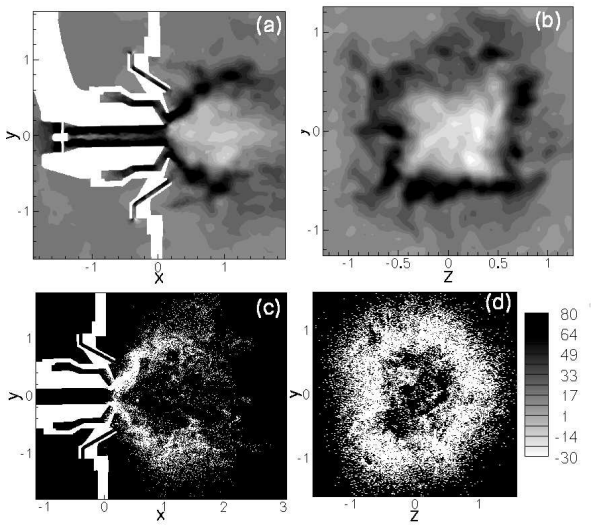

Fig. 2. Instantaneous snapshots of near-injector axial velocity field and spray droplets: (a) axial velocity in $Z/L_{ref} = 0$, (b) axial velocity in $X/L_{ref} = 1.1$, (c) spray droplets in $Z/L_{ref} = 0$, and (d) spray droplets in $X/L_{ref} = 1.1$. Also shown is the color scale for normalized axial velocity.

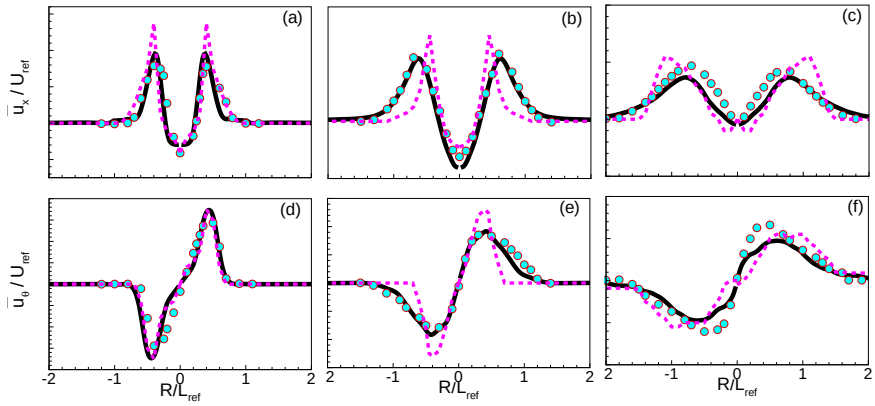

Fig. 3. Radial variation of normalized mean axial and swirl velocity at different axial locations, ∘ experimental data [29], —— LES, ---- RANS: (a,d) $X/L_{ref} = 0.4$, (b,e) $X/L_{ref} = 1.1$, (c,f) $X/L_{ref} = 2.1$.

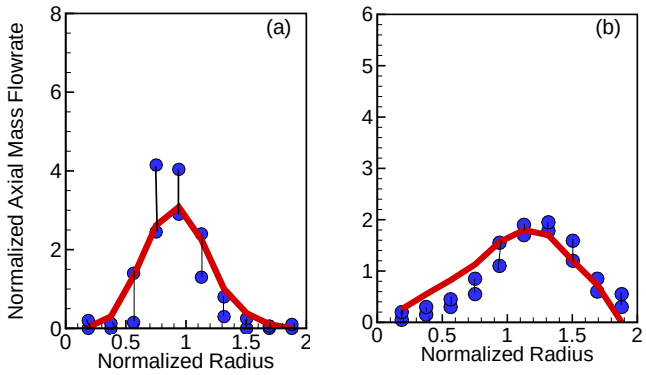

Fig. 4. Comparison of radial variation of normalized liquid axial mass flux at two axial locations, ∘ —— ∘ experimental error bar [29], —— LES: (a) $X/L_{ref} = 1.1$, (b) $X/L_{ref} = 2.1$.

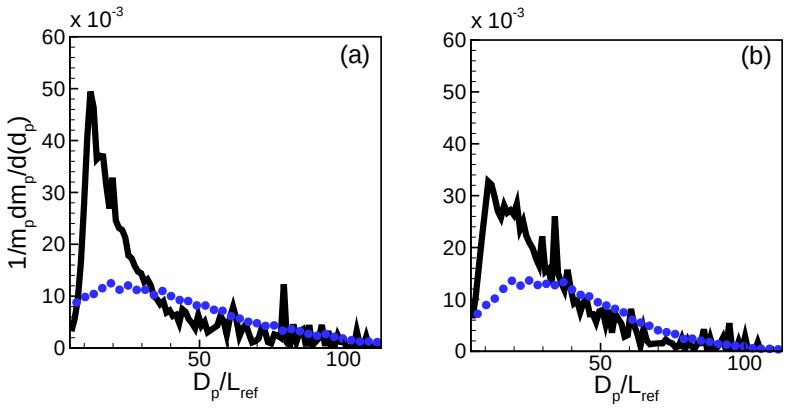

Fig. 5. Comparison of normalized droplet mass-distribution at different axial locations, ∘ experiments [29], —— LES: (a) $X/L_{ref} = 1.1$, (b) $X/L_{ref} = 2.1$.